

Settlement prediction for footings based on stress history from V_S measurements

Hyung Ik Cho^{1a}, Han Saem Kim^{1b}, Chang-Guk Sun^{1c} and Dong Soo Kim^{*2}

¹Earthquake Research Center, Korea Institute of Geoscience and Mineral Resources,
124 Gwahak-ro, Yuseong-gu, Daejeon 34132, Republic of Korea

²Department of Civil and Environmental Engineering, Korea Advanced Institute for Science and Technology,
291 Daehak-ro, Yuseong-gu, Daejeon 34141, Republic of Korea

(Received November 2, 2018, Revised November 18, 2019, Accepted February 5, 2020)

Abstract. A settlement prediction method based on shear wave velocity measurements and soil nonlinearity was recently developed and verified by means of centrifuge tests. However, the method was only applicable to heavily overconsolidated soil deposits under enlarged yield surfaces. In this study, the settlement evaluation method was refined to consider the stress history of the sublayer, based on an overconsolidation ratio evaluation technique, and thereby incorporate irrecoverable plastic deformation in the settlement calculation. A relationship between the small-strain shear modulus and overconsolidation ratio, which can be determined from laboratory tests, was adopted to describe the stress history of the subsurface. Based on the overconsolidation ratio determined, the value of an empirical coefficient that reflects the effect of plastic deformation over the elastic region is determined by comparing the overconsolidation ratio with the stress increment transmitted by the surface design load. The refined method that incorporate this empirical coefficient was successfully validated by means of centrifuge tests, even under normally consolidated loading conditions.

Keywords: settlement; footings; shear wave velocity; overconsolidation ratio; centrifuge modelling

1. Introduction

The stress history of a soil has important effects on its behavior. Clayton *et al.* (1985) reported that the effect of overconsolidation under zero-lateral-yield (K_o) conditions, which might be broadly interpreted in the field, has two important effects on a soil: (a) the yield surface is expanded, so that reload deformation is reduced, and (b) the horizontal stresses are increased above their normally consolidated K_o level. As stress history induces changes in the stress state and deformation characteristics of soil deposits, the effect of the stress history of the ground should be taken into account in settlement prediction for footings.

A settlement prediction method, which is based on shear wave velocity (V_S) measurements and the nonlinearity of soil, was recently proposed by Cho *et al.* (2017). It basically follows Schmertmann's approach (Schmertmann *et al.* 1978), but V_S was utilized, instead of CPT- q_c values (Mir *et al.* 2017) to determine the deformation characteristics of soil, because V_S is directly related to the deformation

characteristics of soil (i.e., the maximum shear modulus, G_o). By combining the V_S measured in the field and the modulus reduction curve measured in the laboratory, the nonlinear deformation characteristics of soil can be described, taking into consideration of the confinement stress and strain level increments. However, Cho *et al.* (2017) commented that this method is only applicable to accounting for the elastic load-settlement response in cases when the plastic deformation of soil layers caused by particle rearrangement cannot be considered. As the basis of the method was the elasticity theory for calculation of settlement, the applicability of the method was inevitably limited to heavily overconsolidated soil deposits with enlarged yield surfaces. In contrast to settlements in soil layers under heavily overconsolidated conditions, settlements that occur under normally consolidated or slightly overconsolidated conditions relative to the surface design load level are largely dependent on the plastic deformation of the particulate media. The plastic behavior should therefore be incorporated in the settlement prediction method to increase the method's applicability.

To better consider the plastic deformation induced in soil layers under normally consolidated loading conditions, the current stress state should be evaluated in advance. This serves to distinguish among loading conditions, such as normally consolidated loading or overconsolidated loading conditions, by comparing the level of stress transmitted to the sublayers as a results of the surface design load with the current stress state of the sublayers. The technique used to evaluate the current stress condition of the soil layers is important. Various studies have been carried out in the

*Corresponding author, Professor

E-mail: dskim@kaist.ac.kr

^aPh.D.

E-mail: hicho@kigam.re.kr

^bPh.D.

E-mail: adoogen@kigam.re.kr

^cPh.D.

E-mail: pungsun@kigam.re.kr

laboratory and field to evaluate the stress conditions of soil layers. However, it can be difficult to obtain reliable results, because of sample disturbance induced during sample acquisition, transportation, and testing (Jamolkowski *et al.* 1985) and because of the technical and cost limitations of the field techniques available (Cho *et al.* 2018).

Because V_S is directly related to the effective stress conditions in the direction of wave propagation and particle motion (Roesler 1979, Yu and Richart 1984, Cho *et al.* 2014), the stress condition of a soil can be non-intrusively captured by V_S measurements. Thus, it is reasonable to expect that evidence of the stress history can be determined from the current stress condition of a soil using V_S . The preconsolidation stress is one of the parameters used to define the stress history of soil deposits. Yoon *et al.* (2011) suggested a method to evaluate the preconsolidation stress using a relationship between V_S and the vertical effective stress ($V_S - \log p'$) and the intersection point of the bilinear line of the $V_S - \log p'$ corresponds to the preconsolidation stress because the slope of the $V_S - \log p'$ curves are different under normally consolidated and overconsolidated conditions. Cho *et al.* (2018) proposed a technique for evaluating the overconsolidation ratio (*OCR*) in the centrifuge model ground based on V_S . A relationship between G_o and *OCR* is established and used to describe the stress history in the centrifuge models subjected to various loading conditions quantitatively.

In this study, the settlement prediction method developed by Cho *et al.* (2017) was refined by considering the stress history of a sublayer based on an *OCR* evaluation for cohesionless sand ground, so that irrecoverable plastic soil deformation can be incorporated in the settlement calculation. A relationship between G_o and *OCR* derived from V_S measurements (Cho *et al.* 2018) is used to describe the stress history of the subsurface. Based on the *OCR* values determined, the value of an empirical coefficient (c) can be determined by comparing the *OCR* with the stress increment transmitted by the surface design load and used to reflect the effect of the plastic deformation over the elastic region. The refined method, using this empirical coefficient, was validated by means of centrifuge tests.

2. Refinement of new settlement prediction method

2.1 New settlement prediction method using V_S

Cho *et al.* (2017) proposed a new settlement prediction method, based on Schmertmann's approach (Schmertmann *et al.* 1978), that combines the strain-dependent modulus derived from V_S , and the strain influence factor profile (I_z) derived from elasticity theory. In this method, the deformation modulus, E_{ij} , of each soil layer is adopted considering both the stress increment by surface design load and strain dependency. The strain dependency is reflected by a function of stress proposed by Fahey (1992). Fahey (1992) suggested that the normalized shear modulus (G/G_o) based on a hyperbolic stress-strain relationship (i.e., Hardin & Drnevich 1972) can be expressed not only as a function of shear strain but also as a function of shear stress. The mobilized modulus can be expressed as follows:

$$E_{ij} = E_{o,j} \left(\frac{\sigma_{ov,j} + q_i I_{z,j}}{\sigma_{ov,j}} \right)^n \left(1 - f \left(\frac{q_i I_{z,j}}{\sigma_{max}} \right)^g \right) \quad (1)$$

where $E_{o,j}$ is the initial small-strain Young's modulus, equal to $E_o = 2G_o(1 + \nu)$; $\sigma_{ov,j}$ is the initial vertical stress at depth z_j ; q_i is the footing load; n is the stress exponent; f and g are model parameters that changes the shape of the stress-strain curve and adjust the model to approach failure at finite strain; and σ_{max} is the ultimate axial bearing capacity.

The term I_z , which was first proposed in conjunction with Schmertmann's method (1970), describes the distribution of the applied load in the subsoil layer with respect to depth. Through the combination with modulus determined from Eq. (1) and the conceptual framework of Schmertmann's method, the total settlement of a footing can be calculated by summation of each sublayer settlement corresponding to the applied stress q_i as follows:

$$s = q_i \sum \frac{I_{zi} \Delta z_i}{E_{o,i} \left(\frac{\sigma_i + q_i I_{zi}}{\sigma_i} \right)^n \left(1 - f \left(\frac{q_i I_{zi}}{\sigma_{max}} \right)^g \right)} \quad (2)$$

2.2 Improvements required for settlement prediction method

The original Schmertmann's method utilizes 1) strain influence factor (I_z), which varies depending on the design load, and 2) modulus, which is uniquely determined regardless of the design load. On the contrary, the method proposed by Cho *et al.* (2017) utilizes 1) a unique I_z from elasticity theory regardless of the design load, and 2) modulus, which varies with the design load. There is a certain limitation to the method proposed by Cho *et al.* (2017). They recognized that the new method was only applicable to accounting for the elastic load-settlement response of vertically loaded footings on granular soils and could not account for plastic deformation caused by particle movement. This means that the deformation behavior of loose soil deposits, such as a deposit in a normally consolidated state, cannot be characterized by this method. Because the method was based on the elasticity theory for calculation of settlement, wherein the moduli of soil layers are considered by means of a load transfer mechanism (i.e., I_z), which can also be calculated from elasticity theory, the applicability of the method is inevitably limited. Cho *et al.* (2017) explained that particle rearrangement, caused by interparticle slip and rotation, governs deformation behavior, rather than the compression of the soil mass related to the modulus under normally consolidated loading conditions (Mesri & Vardhanabhuti 2009). Particle rearrangement has some effect on the coordination number and contact area of the particles (Martin *et al.* 2003, Cho *et al.* 2006), and consequently, has a significant effect on the overall volume of soil layers.

In contrast to settlement that occurs in soils that are subjected to heavily overconsolidated conditions, settlement that occurs under normally consolidated or slightly overconsolidated conditions relative to the surface design load is largely dependent on the plastic deformation behavior of particulate media. Given this, the plastic

behavior should be taken into consideration to increase the applicability of the method. In this study, we sought to develop an approach to consider the plastic deformation that occurs under normally consolidated conditions by introducing an empirical adjustment coefficient (c).

An empirical coefficient has often been employed to improve the accuracy of settlement prediction equations based on elasticity. Burland & Burbidge (1985) suggested the use of empirical coefficients in a settlement prediction method that considers soil compressibility in a manner different for NC and OC deposits suggested by the SPT- N value. Leonards & Frost (1988) also proposed a settlement prediction method based on Schmertmann's conceptual framework. In their method, the settlement or soil stiffness is adjusted using the ratio of the stress increment corresponding to the NC portion and the OC portion in a given layer to the total increment of stress in the layer. In this study, the settlement prediction method proposed by Cho *et al.* (2017) was similarly refined by the introduction of an empirical coefficient (c) related to the stress history of the soil layers to account for the excess settlement caused by plastic deformation over the elastic region (i.e., the yield surface). By comparing the level of the stress increment caused by the surface design load with the stress history for each soil layer, the empirical coefficient (c) profile through the depth can be determined reflecting the loading states.

2.3 OCR evaluation of cohesionless soil using V_S

To evaluate whether the sublayer is subjected to OC loading or NC loading conditions due to the stress increment transmitted by the surface design load, the current stress condition of each soil layer should be estimated. An OCR evaluation technique based on V_S measurements can be utilized for this purpose. Cho *et al.* (2018) proposed a relationship between G_o and OCR based on V_S measurements to describe the stress history of sand models during centrifuge tests. By establishing a relationship for the testing sand, the in-flight stress states of the centrifuge model could be investigated in terms of OCR. For cohesive soils, the G_o is a function of the void ratio (e) and OCR and can be expressed by the well-known Hardin and Richart equation. To improve the applicability of the OCR term in the G_o equation, which was limited to cohesive soils, Cho *et al.* (2018) adopted and verified the following formula to take into account the effect of stress history on G_o , even for cohesionless soils:

$$G_o = A' \cdot F(e) \cdot \left(\frac{\sigma_v'}{1kPa} \right)^{n'} OCR^{k'} \quad (3)$$

where A' is an experimentally determined constant reflecting the soil fabric; n' is an experimentally determined stress exponent; σ_v' is the vertical effective stress; k' is an exponent of the OCR value, which is equivalent to the difference between the stress exponent during loading and unloading that reflects the increment in horizontal stress caused by lateral stress locking during the unloading stage (Choo & Burns 2014); and $F(e)$ is a void ratio function, $F(e) = e^{-1.3}$, as proposed by Lo presti (1989). If the parameters A' , n' , and k' are determined by laboratory testing, such as

oedometer testing, for a certain soil, the OCR can be quantified from V_S measurements. Once the OCR values are obtained for the soil layers, the maximum previous load (i.e., preconsolidation pressure) that has a serious effect on the compressibility of the soils can be determined from elasticity theory. The preconsolidation pressure is the maximum effective stress ever experienced by a particular soil (Becker *et al.* 1987, Burland 1990, Casagrande 1936) at each depth and a pseudoelastic limit that separates "elastic" pre-yield from "plastic" post-yield behavior of a soil (Umar & Sadrekarimi 2016). The OCR evaluation technique is used to evaluate the loading conditions of the ground in the refined settlement prediction method described in a subsequent section.

2.4 Refined settlement prediction method based on stress history

The plastic deformation of each soil layer can be incorporated into the settlement prediction by multiplying the empirical coefficient (c) by the elastically calculated settlement. Details of the procedure for determining the value of the empirical coefficient are presented schematically in Fig. 1. To determine the change in the value of the empirical coefficient (c) with depth, the elastic limit (i.e., the yield surface), which is directly related to the maximum previous vertical stress, should be determined and compared to the profile of the vertical stress increment transmitted by the surface design load.

The elastic limit can be determined separately for shallow depths and deep depths. For deep depths, the elastic limit is calculated by multiplying the evaluated OCR value (i.e., Eq. (3)) by the theoretical vertical effective stress with depth, as indicated in Figure 1a by solid circles. As mentioned previously, the OCR can be estimated from V_S measurements. The smoothed elastic limit profile can be described by a power regression model for the solid points with depth. In cases of shallow depth that governs the total settlement due to its softness, an equivalent-past surcharge load that causes same level of elastic limit, which determined from OCR, at the shallowest point can be estimated from I_z on the basis of elasticity theory, because I_z represents the load transfer mechanism as mentioned earlier. The combination of the estimated equivalent-past surcharge load and the I_z profile produces an elastic limit profile for a shallow depth such as that shown in Figure 1a. The entire elastic limit profile with depth can be drawn by integrating the elastic limit profiles for both shallow and deep depths and then used for precise determination of the yield surfaces of sublayers.

Fig. 1(b) illustrates a comparison between the calculated elastic limit and various profiles of the vertical stress increment transmitted by different levels of the surface design load. This comparison can be conducted in terms of OCR values by normalizing the elastic limit and stress increment by the vertical effective stress at each depth. The induced design stress profile can be represented as the ratio of the stress transmitted by the design load to the current vertical effective stress, i.e., the design OCR. Similarly, the elastic limit can be converted to an OCR term, namely, the ratio of the elastic limit to the current vertical effective

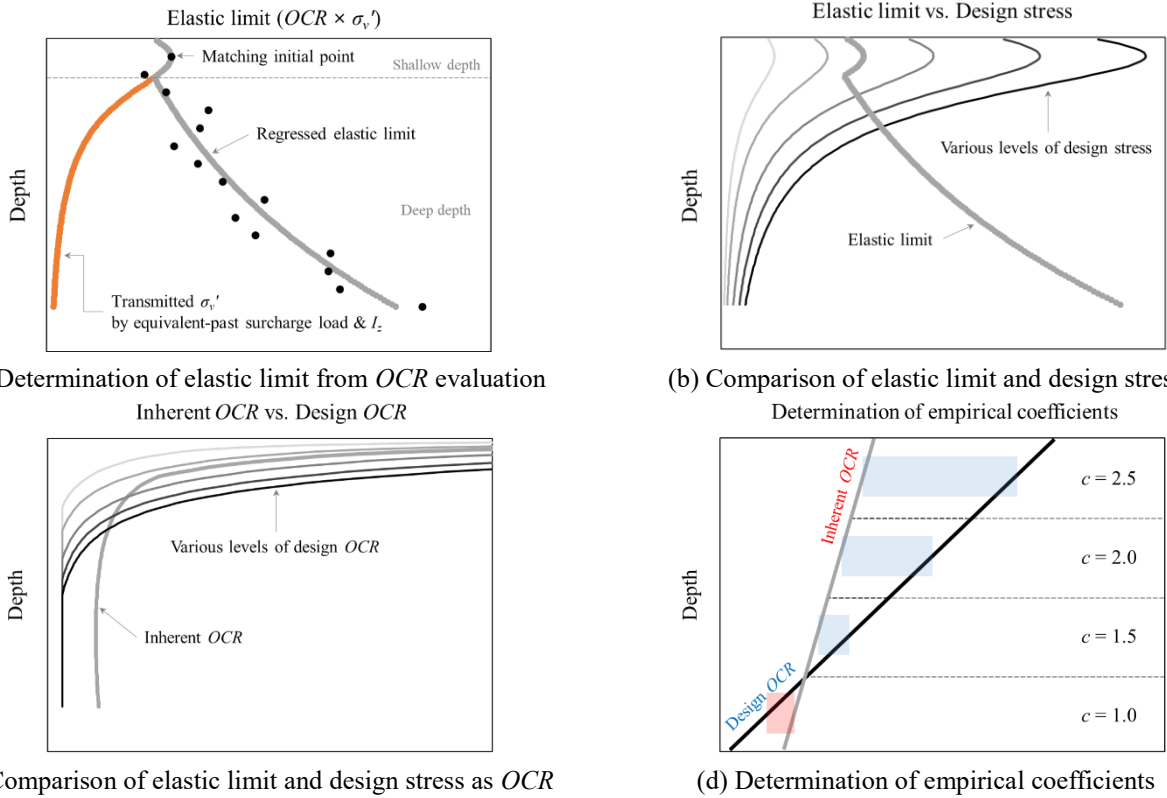


Fig. 1 Schematic diagram for determination of an empirical coefficient (c) value according to the surface design load and stress history of the sublayer

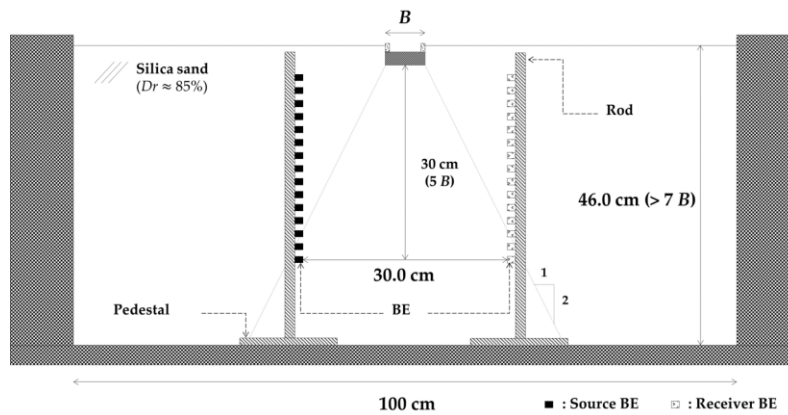


Fig. 2 Centrifuge model configuration (Cho *et al.* 2017)

stress, i.e., the inherent OCR . Fig. 1(c) shows a comparison of two different OCR profiles, such as a profile of an elastic limit and a profile of a vertical stress increment transmitted by various levels of the surface design load. This type of comparison makes it possible to identify more intuitively the deformation characteristics of soil layers as functions of the design load level and depth. Finally, values of an empirical coefficient (c) can be determined based on the difference between the design OCR and the inherent OCR with depth. We tried to set the c value to vary depending on the degree of difference, as shown in Fig. 1(d). The determination of c is described in detail later in the related section. The empirical coefficient c is eventually multiplied by settlements caused by the stress of the NC portion exceeding the elastic limit with depth.

3. Centrifuge study performed by Cho *et al.* (2017)

In this study, the refined settlement prediction method was validated using the centrifuge test results presented by Cho *et al.* (2017). They performed three centrifuge tests and obtained load–settlement curves for footings with various length-to-breadth (L/B) ratios, together with V_S profiles. The experimental procedure and test results are briefly explained herein, and the results are compared with predictions obtained using the refined settlement prediction method.

3.1 Experimental procedure

Centrifuge tests were carried out using model footings with L/B ratios of 1.0, 2.5, and 5.0 to represent square and

rectangular footings. The model footings were made of aluminum and were 60 mm long. Fig. 2 shows a schematic diagram of a model footing constructed on the centrifuge model ground. Dry silica sand (Kim *et al.* 2015) was used as the centrifuge model ground material. Its basic properties have been reported by Cho *et al.* (2017). Fifteen pairs of bender element arrays were installed in the model box to measure the V_S of the model ground during centrifuge tests at a high g-level (Kim & Kim 2010). The model ground was constructed using a dry compaction method, and the final relative density (D_r) of the prepared model ground was approximately 85%.

The centrifuge tests were conducted at a target g-level of 40, and model footings with prototype lengths of 2.4, 6.0, and 12.0 m were simulated, according to the scaling law (Tasiopoulou *et al.* 2015), respectively. Vertical loading was applied to the top of each model footing. After the first loading, the load was completely removed, and a second loading of a larger magnitude than the first loading was then applied. Before each vertical loading, the V_S beneath the footings was measured using the bender elements.

3.2 Determination of input parameters for predictions

To facilitate precise predictions from the point-based measured V_S profiles, interpolation based on the least

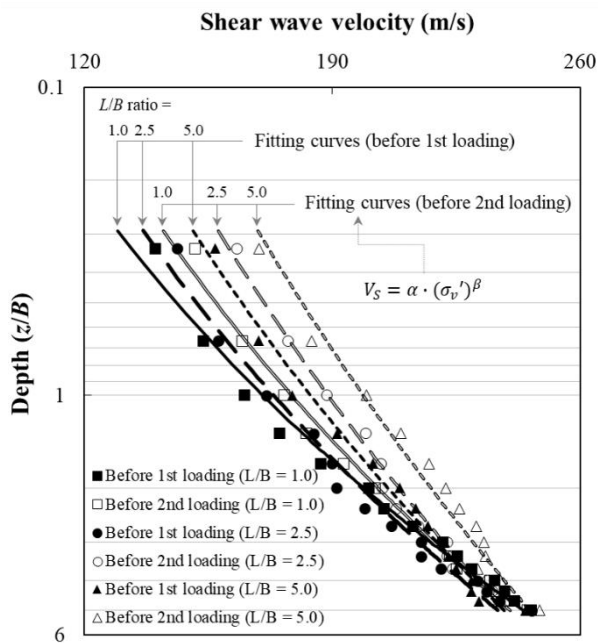


Fig. 3 Shear wave velocity profiles obtained for three models

Table 1 Soil parameters for settlement prediction (Cho *et al.* 2017)

f	g	n	Poisson Ratio, ν	Friction Angle, θ	Bearing Capacity, σ_{max}
0.96	0.09	0.5	0.2	43°	$L/B = 1.0, 3439 \text{ kPa}$
					$L/B = 2.5, 2729 \text{ kPa}$
					$L/B = 5.0, 2506 \text{ kPa}$

squares method was used to produce continuous V_S profiles. Fig. 3 shows the interpolated V_S profiles with respect to depth (Kim *et al.* 2017), normalized by the footing breadth (B) for the three experiments. Note that the V_S measured before the second loading became greater than the first loading and that the depth at which V_S increased with the L/B ratio.

To compare the load–settlement curves from the centrifuge tests with predicted values, Cho *et al.* (2017) applied a profile of a strain influence factor (I_z) based on elasticity theory. The soil parameters that are required in Eq. (2) to describe the nonlinear deformation characteristics of soils were determined based on a literature review and triaxial (TX) test results for the silica sand. The results are tabulated in Table 1.

The V_S profile measured before each loading was used in each settlement prediction to represent a reasonable initial stress state for the model ground. The V_S can be converted to elastic modulus required in Eq. (2) utilizing unit weight and Poisson’s ratio. The nonlinear deformation characteristics of the soil with respect to the confinement stress and strain increase was considered using the parameter values presented in Table 1.

3.3 Comparisons of load-settlement curves with predictions

Fig. 4 show comparisons by Cho *et al.* (2017) of the measured model settlements with the predictions from the original version of the settlement prediction method for L/B ratios of 1.0, 2.5, and 5.0, respectively. The settlements of the model footings were normalized with respect to the footing breadth (B).

The centrifuge test results for the first loading indicated a very soft deformable foundation in comparison to the two predictions, regardless of the L/B ratio. Cho *et al.* (2017) reasoned that for the first loading, the particle rearrangement caused by interparticle slip and rotation governed the deformation behavior, rather than the compression of the soil mass related as a function of the modulus. According to this reasoning, irrecoverable plastic behavior caused by particle rearrangement starts in a very small strain region, and elastoplastic behavior of the soil then emerges beyond a very small elastic limit.

In contrast, the centrifuge test results and two predictions for the second loading revealed different trends. The predictions for the three cases based on I_z from elasticity theory yielded good agreement with the centrifuge test results, especially up to the settlements corresponding to the maximum previous loadings. The yield points (elastic limits) of the three model grounds increased as a results of the maximum previous loading of the first loading cycle (Schanz *et al.* 1999). Note that major particle rearrangement occurred and disappeared during the first loading cycle. It can be seen that the unique I_z used in conjunction with the initial elastic modulus converted from the measured V_S before second loading reasonably defines the deformation behavior in the elastic region.

However, the predictions underestimated the settlements of the model footing after the maximum previous loading in the second loading stage. The predictions and load-

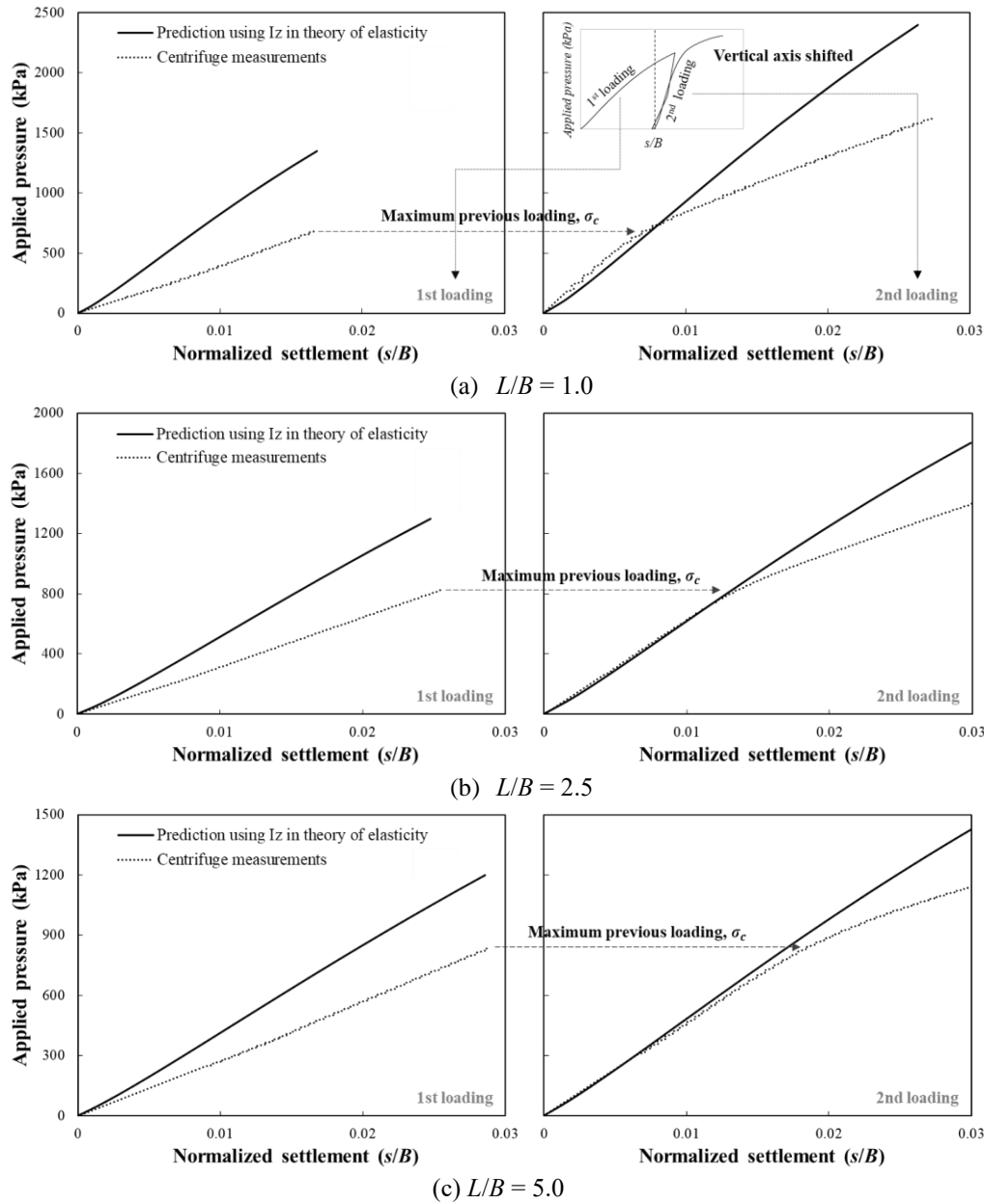


Fig. 4 Comparisons of load-settlement curves with original predictions (left side: first loading; right side: second loading) (Cho *et al.* 2017)

settlement curves from the centrifuge tests exhibited greater discrepancies, as in the case of the first loading stage. Because modeling of soil behavior utilizing the stiffness is valid up to the elastic limit, it is not possible that the original method based on the hyperbolic stress-strain model estimates the soil deformation behavior under an NC stress state (i.e., beyond the maximum previous loading) governed by relative particle movements. For this reason, Cho *et al.* (2017) limited the applicability of the original version of the method to heavily overconsolidated deposits and pointed out the necessity of employing empirical coefficients to account for plastic deformation behavior under normally consolidated loading conditions in further studies.

4. Application of the refined settlement prediction method

The centrifuge test results described in the previous section were compared with the results obtained from the settlement prediction method refined by considering the stress history of the centrifuge model ground from V_S measurements.

4.1 OCR evaluation of centrifuge model using V_S

The stress history of the centrifuge model ground was evaluated first using a G_o -OCR relationship (Eq. (3)) based on V_S measurements. As the G_o -OCR relationship was

Table 2 Soil parameters for OCR evaluations

A' (kPa)	n'	k'
3020.8	0.51	0.21

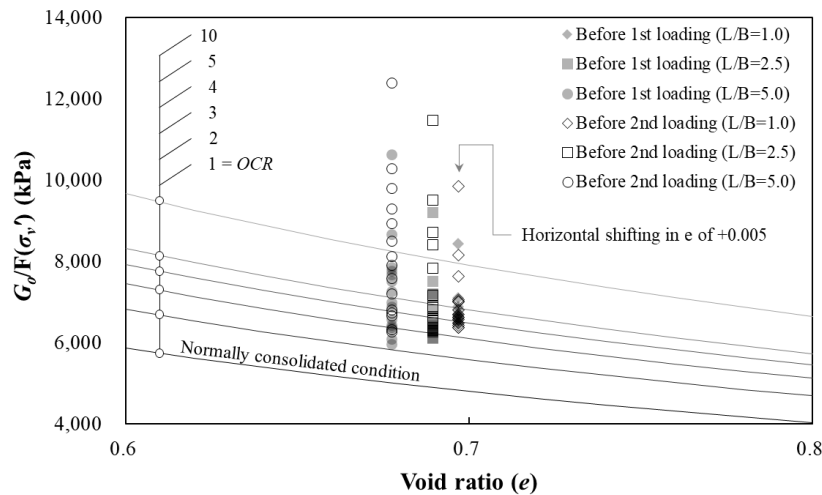


Fig. 5 Determination of stress history of centrifuge models based on the relationship between normalized G_o and void ratio of the testing sand

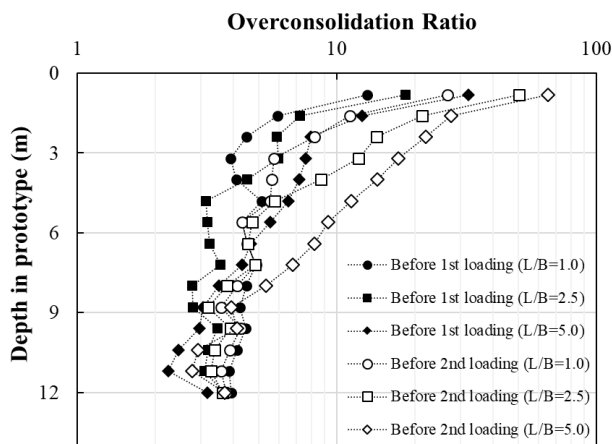


Fig. 6 OCR evaluation of three centrifuge models with depth

established for the silica sand that was used to construct the centrifuge model, according to Cho *et al.* (2018), the V_s profiles measured during the centrifuge tests (see Fig. 3) could be adopted directly for use in OCR evaluation of the centrifuge model ground with depth. The coefficients evaluated for Eq. (3) of the silica sand are tabulated in Table 2. The degree of stress history was analyzed based on the normalized G_o - e (void ratio) graph, using Eq. (3) for the stress state before the first and second loadings, as shown in Fig. 4. In the figure, the stress state of the centrifuge model grounds can be clarified in terms of OCR because the G_o is normalized with respect to the vertical effective stress to determine the degree of horizontal stress caused by the stress history (Mayne & Kulhawy 1982). Each point indicates the stress state at a certain depth, and the solid and open points correspond to the stress states before the first loading and second loading, respectively. It is assumed that the void ratio remained during the loading and unloading sequences. The void ratio of the model for an L/B ratio of 1.0 was shifted slightly to the right to avoid overlapping of the data.

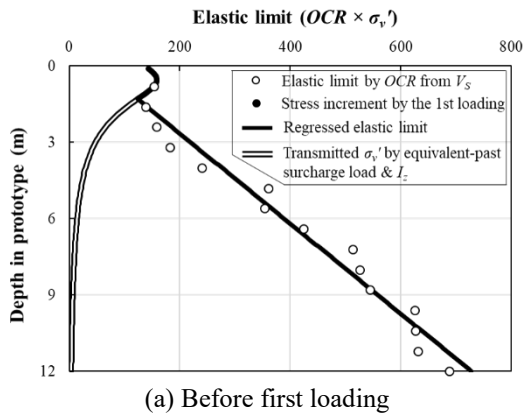
As previously mentioned, three centrifuge model

grounds were constructed by dry compaction at 1 g, and this resulted in a stress history even before the first load application at a centrifugal g -level of 40. After the first loading and unloading of surcharge load on the top of the model ground, the effect of the surcharge load on the stress state of sublayer can be shown by open points. As expected, the OCR of the model ground before the second loading increased because of the residual stress induced during the loading and unloading sequences of the first loading.

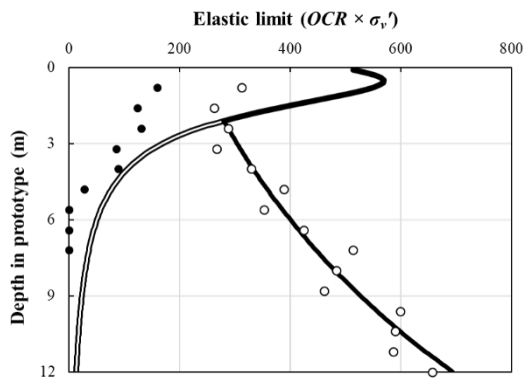
Fig. 6 shows OCR values with prototype depth for each centrifuge model, based on the data points on Fig. 4. The X-axis representing the OCR is on a logarithmic scale. The OCR values are greater at shallow depths, while the OCR values decrease as the depth becomes deeper for the three models. Because high centrifugal acceleration at a target g -level produces in the model ground a stress condition N times higher, according to the scaling law, the effect of compaction energy at 1 g decreases as the depth becomes deeper. After the first load is applied and removed, the OCR of the models was increased, especially at shallower depths. Note that the magnitudes of the first loading (i.e., surcharge load) were 680 kPa, 824 kPa, and 836 kPa for L/B ratios of 1.0, 2.5, and 5.0, respectively. The increasing tendency of the OCR after the first loading is dependent on the L/B ratio. As the L/B ratio increases, the depth at which the OCR increased also increases. This suggests that the load transfer mechanisms to the sublayers from the surface load can be defined according to the L/B ratio. More details are discussed later.

4.2 Determination of empirical coefficients (c) values with depth

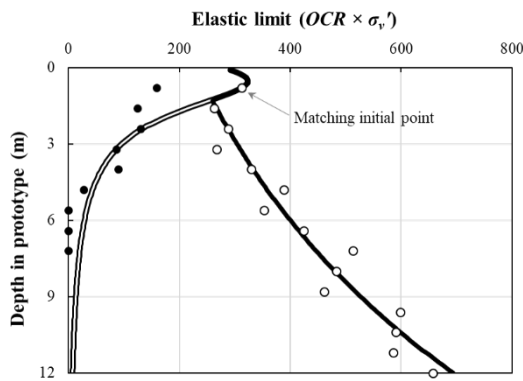
The elastic limit profile can be determined by multiplying the calculated OCR value by the theoretical vertical effective stress with depth for shallow depths and deep depths separately. The elastic limit converted from the OCR at a shallow depth can yield a solution for the equivalent-past surcharge load through backward calculation using I_z from elasticity theory, as mentioned before. This means that the equivalent-past surcharge load



(a) Before first loading

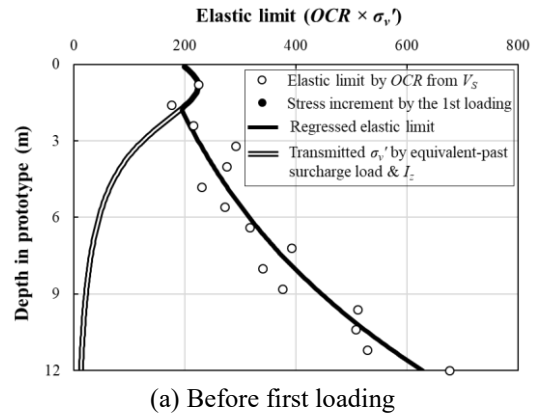


(b) Before second loading using surcharge load actually applied

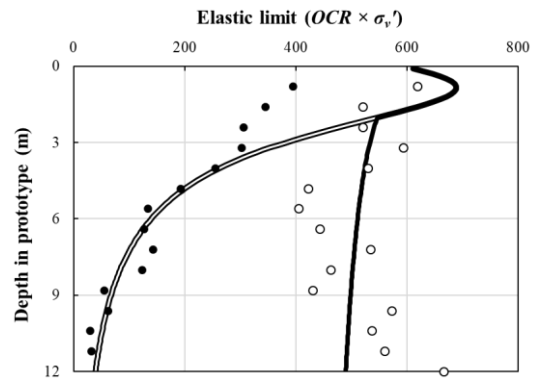


(c) Before second loading using estimated equivalent-past surcharge load

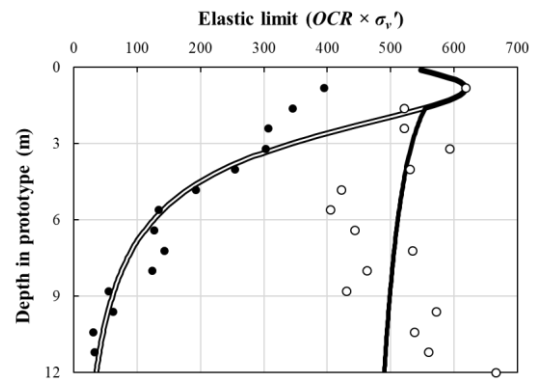
Fig. 7 Determination of elastic limit of model ground for L/B ratio of 1.0



(a) Before first loading



(b) Before second loading using surcharge load actually applied



(c) Before second loading using estimated equivalent-past surcharge load

Fig. 8 Determination of elastic limit of model ground for L/B ratio of 2.5

can be ‘estimated’ based on OCR evaluation of the sublayer. On the other hand, because the surcharge load ‘actually applied’ during the first loading is a known value, the surcharge load estimated from the OCR and that actually applied during tests can be employed separately to determine the elastic limit for a shallow depth.

Figs. 7, 8 and 9 illustrate the elastic limit profiles obtained for each model ground before the first and second loadings. Figs. 7(a), 8(a) and 9(a) are the elastic limit profiles before the first loading. Before the first load is applied to a centrifuge model, the only stress history that the model ground experiences, is compaction at 1 g . Therefore, only the estimated equivalent-past surcharge load is available for use in the determination of the elastic

limit. Figs. 7(b), 8(b) and 9(b) show the elastic limit profiles determined before the second loading using the surcharge load actually applied during the tests, while Figs. 7(c), 8(c) and 9(c) show those determined using the surcharge load estimated from the OCR . Note that the size of the elastic limit is different for the two different surcharge loads. The elastic limit determined using the surcharge load estimated from OCR evaluation is identical to the elastic limit determined from the OCR because the surcharge load itself was determined from the OCR . It was expected that the different sizes of elastic limits would affect the settlements of the footings.

Application of I_z from elasticity theory can be validated by two types of evidence based on the shape of the elastic

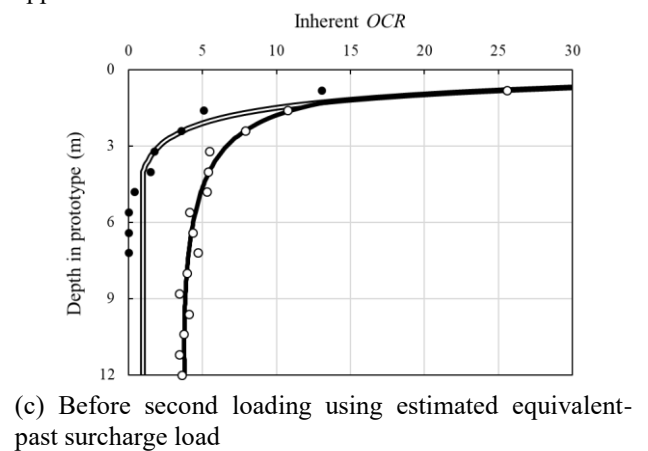
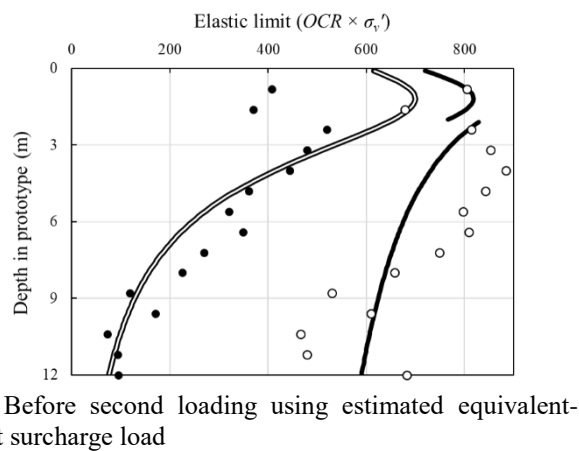
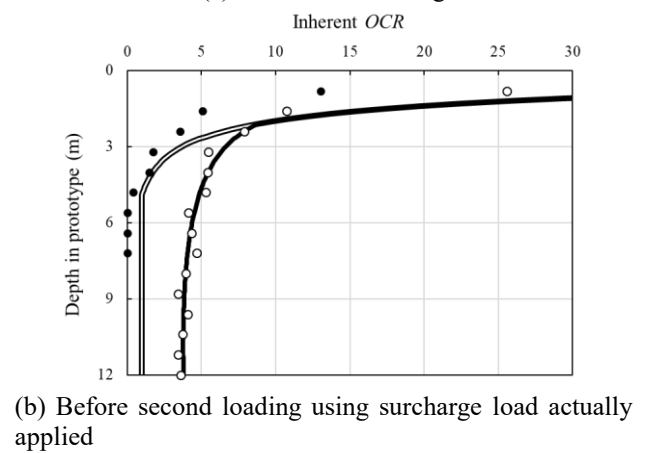
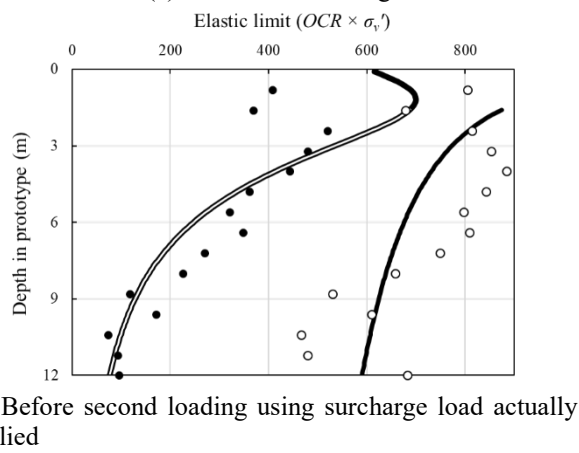
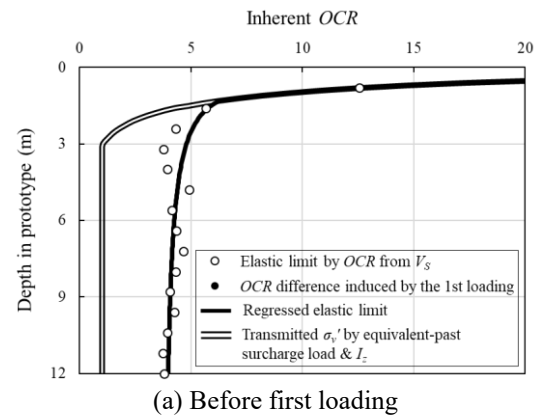
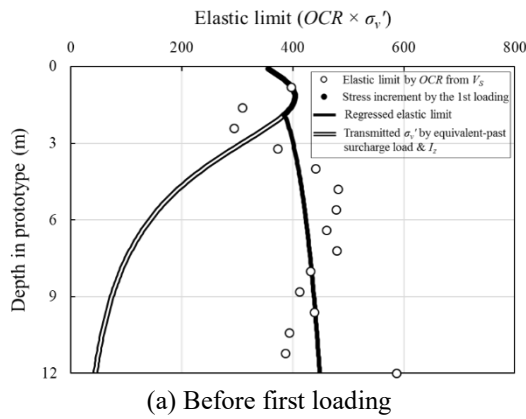


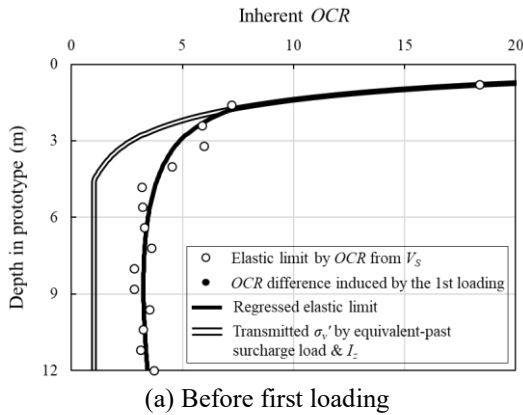
Fig. 9 Determination of elastic limit of model ground for L/B ratio of 5.0

Fig. 10 Determination of inherent OCR of model ground for L/B ratio of 1.0

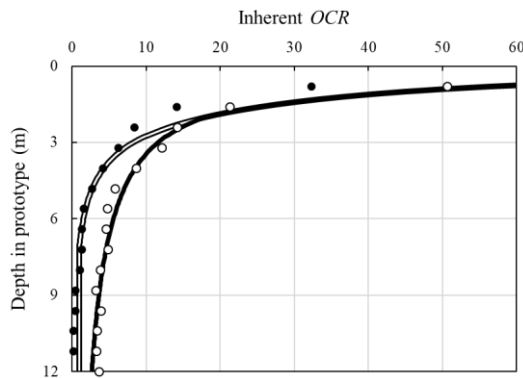
limit profiles determined. First, the elastic limit profiles of the model grounds before the second loading moved to the right, especially for shallow depths, relative to those before the first loading, as a result of OCR changes caused by application and removal of the first loading, whereas the elastic limit profiles of the model grounds before the first loading increased with depth. As the L/B ratio increased, the enlarged area became deeper. This phenomenon is similar to that indicated by the concept of I_z from elasticity theory that suggests that the depth influenced by I_z increases with increasing L/B ratio. Second, the solid points in parts b and c of Figs. 7, 8, and 9 are comparable to the stress transmitted by the surcharge load with the I_z from elasticity theory. The solid points result from the differences in the

OCR s of the model grounds before the first and second loadings, these differences understandably having been caused by the first loading. The points decrease with depth, but the trend differs depending on the L/B ratio, as does the shape of I_z .

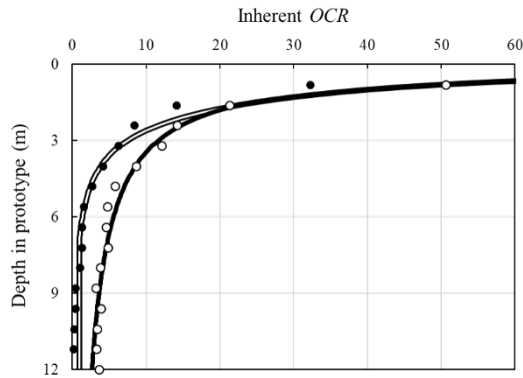
Figs. 10, 11 and 12 show elastic limit profiles of the three model grounds in terms of OCR . As explained earlier, the stress profile caused by the surface design load and the elastic limit can be compared in terms of OCR values because the design stress can be expressed as a ratio of the stress transmitted by the surface design load to the current vertical effective stress, i.e., the design OCR . The elastic limit expressed as an OCR was previously defined as the inherent OCR and can be evaluated from V_s measurements



(a) Before first loading

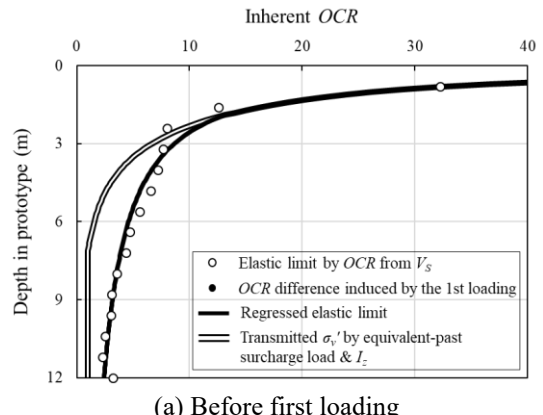


(b) Before second loading using surcharge load actually applied

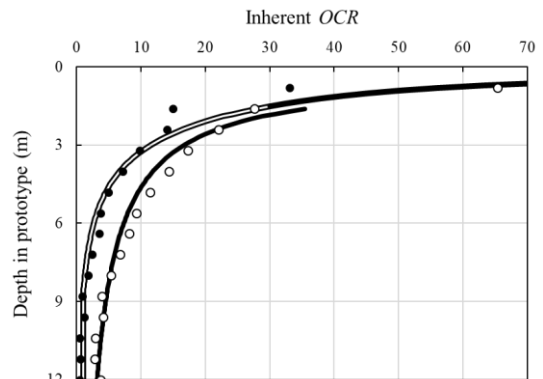


(c) Before second loading using estimated equivalent-past surcharge load

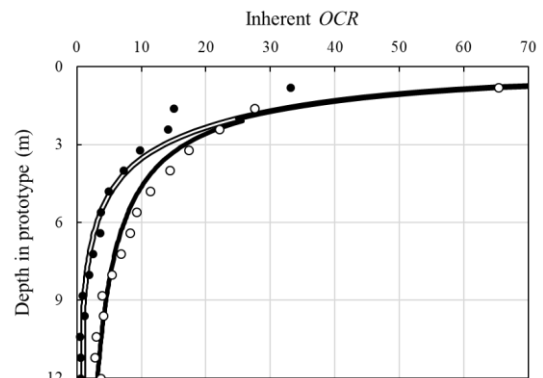
Fig. 11 Determination of inherent OCR of model ground for L/B ratio of 2.5



(a) Before first loading



(b) Before second loading using surcharge load actually applied



(c) Before second loading using estimated equivalent-past surcharge load

Fig. 12 Determination of inherent OCR of model ground for L/B ratio of 5.0

with depth, as shown in the figures. The solid points represent the difference in terms of OCR induced by the first loading and OCR profiles transmitted by the equivalent-past surcharge load with I_z . As mentioned before, I_z from elasticity theory reasonably characterizes the stress induced by the surcharge load as a function of the L/B ratio with depth.

Comparison of the inherent OCR and design OCR makes it possible to determine values of the empirical coefficients (c) with depth. Fig. 13 shows an example. In the figure, the inherent OCR of the centrifugal model before the second loading for an L/B ratio of 1.0 (Fig. 10(b)) is compared to the design OCR determined for a surface design load of 1,000 kPa. By comparison, the empirical

coefficient values can be determined based on OCR difference between the inherent OCR and the design OCR. In this study, the empirical coefficients were set according to an interval of the OCR difference of 5 to increase usability and simplicity. As presented in Table 3, four options were selected for the empirical coefficients, and each option was set to have a difference of 0.5 or 1.0 for the two or three OCR intervals. The four options were compared with the results of the centrifuge tests to determine the case-specific empirical coefficients. The three load-settlement curves of the second loading were used, where the effect of the preconsolidation pressure by the first loading and unloading is dominant. In addition, the

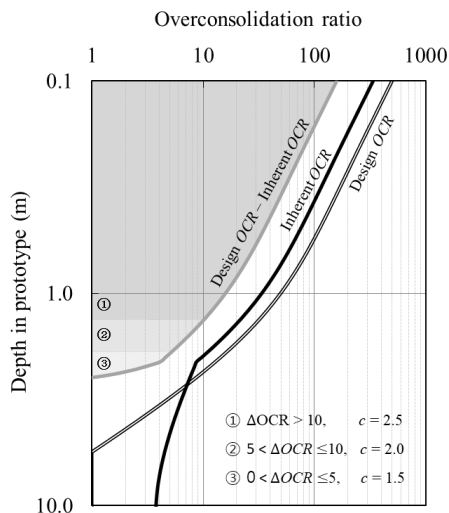


Fig. 13 Determination of empirical coefficients based on the level of difference between inherent OCR and design OCR with depth

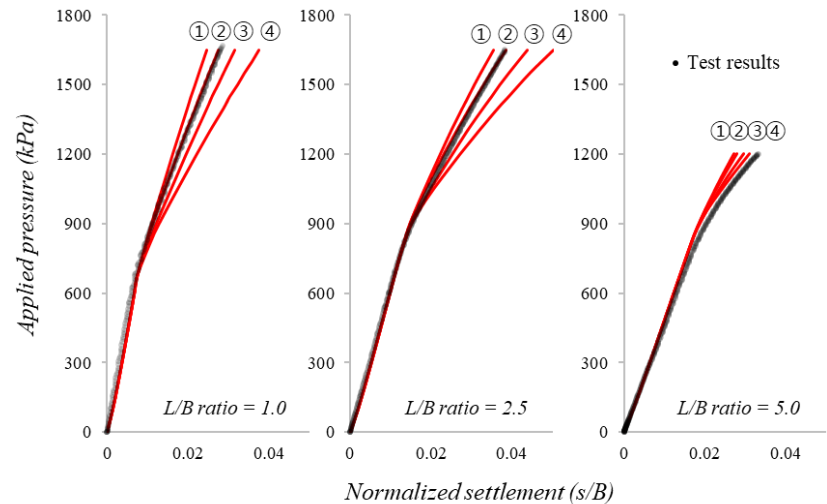


Fig. 14 Four options for determination of empirical coefficients

Table 3 The empirical coefficient options according to the stress state

		Empirical coefficient (c) options			
Option		①	②	③	④
Inherent OCR	0 ~ 5	1.5	1.5	2.0	2.0
	5 ~ 10		2.0		3.0
- Design OCR	10 ~	2.0	2.5	3.0	4.0

surcharge load ‘actually applied’ was only applied for the determination of the empirical coefficient to improve accuracy. Fig. 14 compares the load-settlement curves determined with each option presented in Table 3 with the centrifuge test results. Due to the application of the four options, the predictions show a bilinear tendency similar to the test results. Based on the OCR difference of 5, the interval of 1.0 in the empirical coefficients (options 3, 4) overestimates the settlements, but the interval of 0.5 over two sections of the OCR difference (option 1) underestimate the settlements. Therefore, the interval of 0.5 in empirical coefficient over three sections was determined case-specifically based on the OCR difference of 5. In Fig. 14, the test result with L/B ratio of 5 was not considered in the empirical coefficient determination because the deflection of the model footing caused by its relatively long length and corresponding lesser stiffness was reflected in the amount of settlements.

4.3 Comparisons of load-settlement curves with predictions

The empirical coefficient (c) is only multiplied by settlements caused by stress from the NC portion exceeding the elastic limit at each depth. The settlements predicted by the refined method using the empirical coefficients were compared with the centrifuge test results, as shown in Figs. 15, 16, and 17 for the three L/B ratios considered. The original predictions by Cho *et al.* (2017), which were shown in Fig. 4, are also shown in these figures. As mentioned

previously, the equivalent-past surcharge load can be estimated based on an OCR evaluation of the sublayers, and the surcharge load actually applied during testing can be used to establish the inherent OCR . On the other hand, only the estimated equivalent-past surcharge load is applicable to centrifuge model grounds before the first loading, considering the effect of compaction at a 1 g level, whereas both the estimated and applied equivalent-past surcharge load can be utilized in settlement prediction for the second loading, because of the information of the first loading. Given that the information on the preconsolidation load is uncertain in most of the in-situ sites, it is expected that the technique based on the ‘estimated’ equivalent-past surcharge load would be better in field application.

The predictions obtained by the refined method for the first loading were similar to the original predictions. The settlements predicted by the refined method indicate high compressibility up to a certain equivalent-past surcharge load and then exhibit slopes comparable to those of the centrifuge test results. As the equivalent-surcharge loads estimated from the OCR are greater, the predictions obtained by the refined method result in some discrepancies with the test results. However, it was confirmed that the difference was significantly reduced.

The predictions obtained by the refined method for the second loading match the real load-settlement curves well, even after the maximum previous loads, whereas the original method underestimates the settlements for normally consolidated loading conditions. The predictions obtained using the actual surcharge load yield more accurate load-settlement curves than those obtained using the equivalent-past surcharge load estimated from OCR values especially for an L/B ratio of 1.0. In the case of a square footing, the sublayer zone influenced by the surface load is narrow and shallow, whereas the ‘tip-to-tip’ distance between the source and receiver Bender elements was identical (30 cm) for the three cases. Therefore, the measured V_s for the square footing could not fully reflect the effect of the stress transmitted by the surface load because the V_s averages the

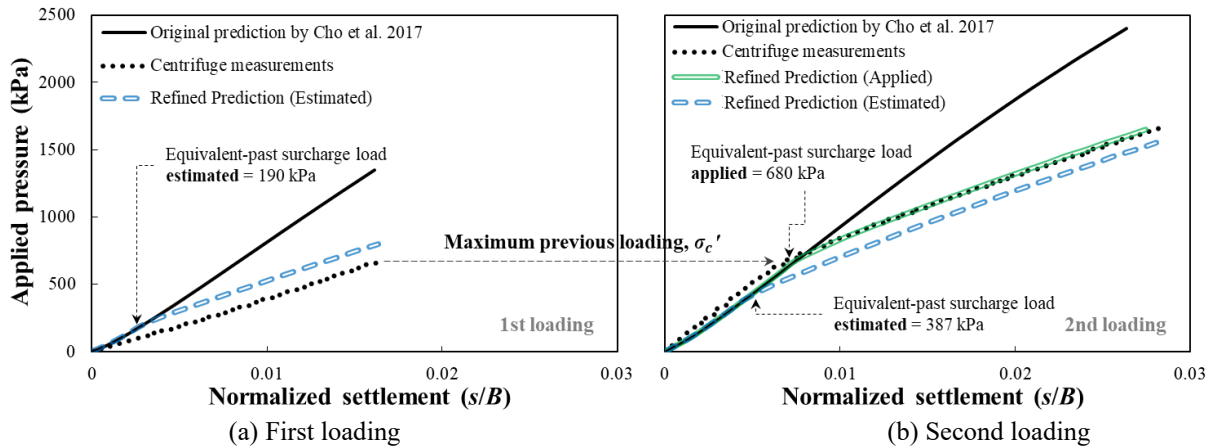


Fig. 15 Comparisons of load-settlement curves with refined predictions ($L/B = 1.0$)

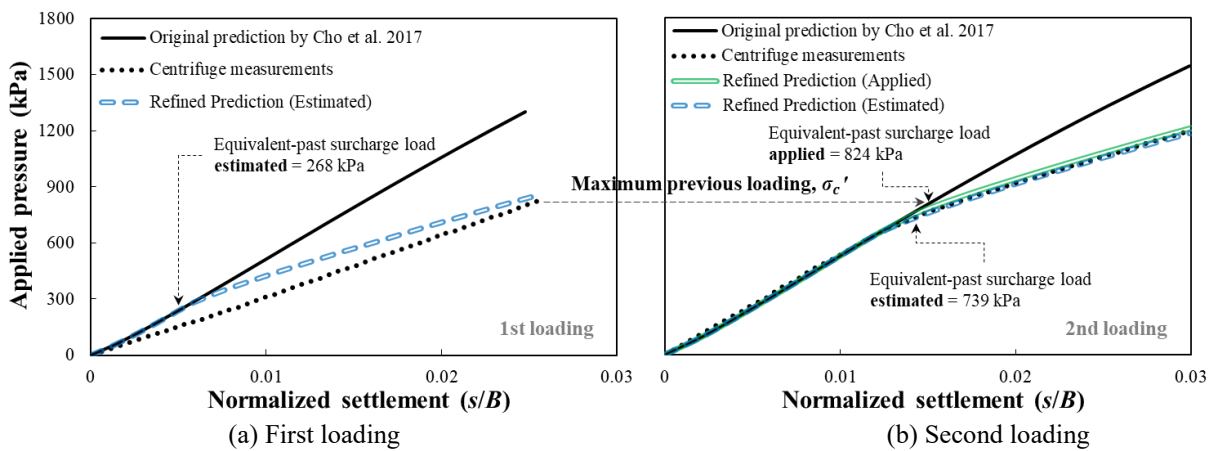


Fig. 16 Comparisons of load-settlement curves with refined predictions ($L/B = 2.5$)

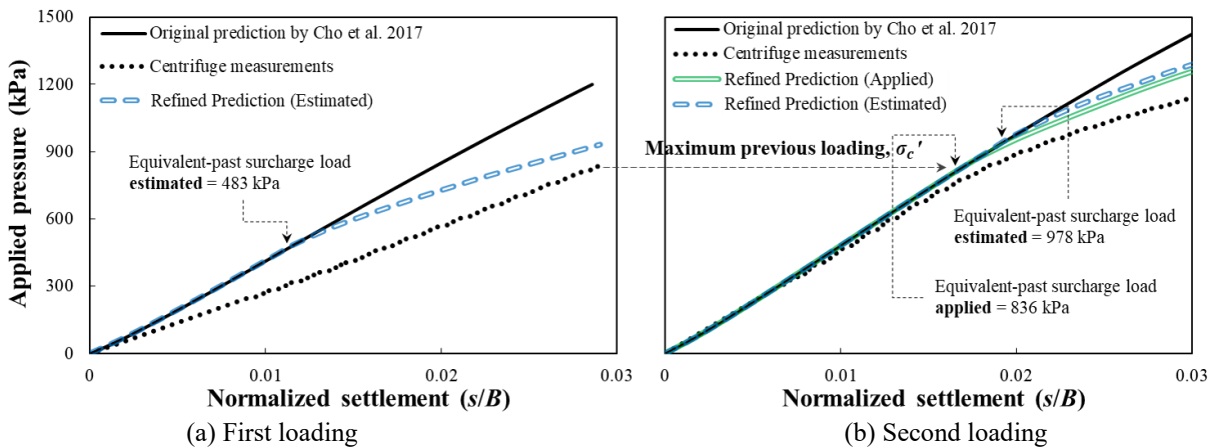


Fig. 17 Comparisons of load-settlement curves with refined predictions ($L/B = 5.0$)

properties within the range. The ‘tip-to-tip’ distance between bender elements has to be adjusted based on the size of the footings.

In the case of L/B ratio of 2.5 and 5.0, there were very small differences in the load-settlement curves obtained using the two different surcharge loads, and the predictions yielded good agreement with the test results for the entire response range. On the other hand, the predicted behavior for the L/B ratio of 5.0 was slightly stiffer than the real behavior observed. This can be attributed to additional

settlement caused by deformation of the model footing itself, which had a length of 30 cm. Although the model footing was made of aluminum so that it would be rigid relative to the stiffness of the model ground, the footing exhibited some deflection in the direction of loading because of its slenderness ratio. If this effect is accurately reflected in the settlement, the refined prediction will predict the phenomenon better, as it does for an L/B ratio of 2.5. In summary, the refined settlement prediction method incorporating an empirical coefficient (c) resulted in better

agreements with the centrifuge testing results than the original predictions by Cho *et al.* (2017) even for normally consolidated loading conditions.

5. Conclusions

This paper proposes a refinement of the settlement prediction method proposed by Cho *et al.* (2017). As the applicability of that method was limited to heavily consolidated soil deposits, given the basis of the method (theory of elasticity based on Schmertmann's framework), plastic deformation under normal to slightly overconsolidated loading conditions could not be considered. To refine the original method, the stress history of soil sublayers was evaluated using V_S measurements, and an empirical coefficient (c) was adopted to consider plastic deformation. The new procedures incorporated into the refined method and the validation of the refined method by centrifuge tests can be summarized as follows:

i) The settlement prediction method proposed by Cho *et al.* (2017) was only applicable to accounting for elastic load–settlement response; plastic deformation of soil layers caused by irrecoverable particle movement could not be considered because the method was based on elasticity theory. In contrast to settlements that occur in soil layers under heavily overconsolidated conditions, settlements that occur under normally consolidated or slightly overconsolidated conditions are largely dependent on the plastic deformation behavior of particulate media. To increase the applicability of the method, the plastic deformation that occurs under normally consolidated loading conditions was incorporated in the settlement prediction by considering a V_S -based stress history evaluation. An empirical coefficient (c) that reflects the effect of the plastic deformation with depth was incorporated by comparing the stress history with the stress transmitted by surface design load.

ii) To evaluate the stress state of a sublayer, which has a significant effect on the sublayer's deformation characteristics, relative to the stress increment caused by the surface design load, the original stress state of each soil layer was estimated based on V_S measurements. In this study, the V_S -based method proposed by Cho *et al.* (2018) was utilized to determine the stress history of centrifuge models. The V_S -based OCR evaluation technique requires the incorporation of laboratory studies of the soil that generate three additional parameters for a G_o - OCR relationship. By establishing the G_o - OCR relationship for the testing sand, the in-flight stress states of centrifuge models were determined in terms of the OCR . The stress state of sublayer is referred to as the inherent OCR and represents the ratio of the past maximum vertical stress to the current vertical effective stress.

iii) The inherent OCR can be compared to the vertical stress increment transmitted by the surface design load. The induced stress profile was defined as the ratio of the stress transmitted by the design load to the current vertical effective stress, i.e., the design OCR . This comparison makes it possible to determine more intuitively the deformation characteristics of soil layers depending on the level of the design load and the depth. The empirical

coefficient (c) value can be determined as a function of the difference between the inherent OCR and the design OCR at each depth. We proposed a means to allow the c value to vary empirically, depending on the degree of difference. The empirical coefficient is eventually multiplied by the settlements caused by the stress of the NC portion over the elastic limit at each depth for the purpose of considering plastic deformation.

iv) The results of centrifuge tests conducted by Cho *et al.* (2017) were used to validate the refined settlement prediction method. Unlike the original method, which underestimated the load–settlement behavior under normally consolidated loading, the refined prediction method yielded good agreement with the centrifuge test results even under normally consolidated loading conditions. Whereas the original settlement prediction method determines the moduli of soil layers on the basis of the confinement stress and strain level increments determined using V_S , the refined settlement prediction method has improved applicability because it incorporates consideration of the plastic deformation behavior that occurs under normally consolidated loading conditions, through an evaluation of the stress history that is also based on V_S . Meanwhile, since the verification of the refined method was carried out on sandy soil, the application to clayey soil requires further validation.

Acknowledgments

This research was supported from Basic Research Project of Korea Institute of Geoscience and Mineral Resources (KIGAM).

References

- Becker, D.E., Crooks, J.H.A., Been, K. and Jefferies, M.G. (1987), "Work as a criterion for determining in situ and yield stresses in clays", *Can. Geotech. J.*, **24**(4), 549-564. <https://doi.org/10.1139/t87-070>.
- Burland, J.B. and Burbidge, E. (1985), "Settlement of foundations on sand and gravel", *Proc. Inst. Civ. Eng.*, **76**, 1325-1381. <https://doi.org/10.1680/iicep.1985.1058>.
- Burland, J.B. (1990), "On the compressibility and shear strength of natural clays", *Géotechnique*, **40**(3), 329-378. <https://doi.org/10.1680/geot.1990.40.3.329>.
- Casagrande, A. (1936), "Determination of preconsolidation load and its practical significance", *Proceedings of the 1st International Conference on Soil Mechanics and Foundation Engineering*, Cambridge, Massachusetts, U.S.A., June.
- Cho, G.C., Dodds, J. and Santamarina, J.C. (2006), "Particle shape effects on packing density, stiffness, and strength: Natural and crushed sands", *J. Geotech. Geoenviron. Eng.*, **132**(5), 591-602. [https://doi.org/10.1061/\(ASCE\)1090-0241\(2006\)132:5\(591\)](https://doi.org/10.1061/(ASCE)1090-0241(2006)132:5(591)).
- Cho, H.I., Park, H.J., Kim, D.S. and Choo, Y.W. (2014), "Evaluation of K_o in centrifuge model using shear wave velocity", *Geotech. Test. J.*, **37**(2), 255-267. <https://doi.org/10.1520/GTJ20130060>.
- Cho, H.I., Kim, N.R., Park, H.J. and Kim, D.S. (2017), "Settlement prediction of footings using V_S ", *Appl. Sci.*, **7**(11), 1105. <https://doi.org/10.3390/app7111105>.
- Cho, H.I., Sun, C.G., Kim, J.H. and Kim, D.S. (2018), " OCR evaluation of cohesionless soil in centrifuge model using shear

- wave velocity”, *Geomech. Eng.*, **15**(4), 987-995.
<https://doi.org/10.12989/gae.2018.15.4.987>.
- Choo, H. and Burns, S.E. (2014), “Effect of overconsolidation ratio on dynamic properties of binary mixtures of silica particles”, *Soil Dyn. Earthq. Eng.*, **60**, 44-50.
<https://doi.org/10.1016/j.soildyn.2014.01.015>.
- Clayton, C.R.I., Hababa, M.B. and Simons, N.E. (1985), “Dynamic penetration resistance and the prediction of the compressibility of a fine-grained sand - a laboratory study”, *Geotechnique*, **35**(1), 19-31.
<https://doi.org/10.1680/geot.1985.35.1.19>.
- Fahey, M. (1992), “Shear modulus of cohesionless soil: Variation with stress and strain level”, *Can. Geotech. J.*, **29**(1), 157-161.
<https://doi.org/10.1139/t92-017>.
- Hardin, B.O. and Drnevich, V.P. (1972), “Shear modulus and damping in soils: Design equations and curves”, *J. Soil Mech. Found. Div.*, **98**(sm7).
- Jamiolkowski, M. (1985), “New developments in field and laboratory testing of soil”, *Proceedings of the 11th International Conference on Soil Mechanics*, San Francisco, California, U.S.A., August.
- Kim, J.H., Choo, Y.W., Kim, D.J. and Kim, D.S. (2015), “Miniature cone tip resistance on sand in a centrifuge”, *J. Geotech. Geoenviron. Eng.*, **142**(3), 04015090.
[https://doi.org/10.1061/\(ASCE\)GT.1943-5606.0001425](https://doi.org/10.1061/(ASCE)GT.1943-5606.0001425).
- Kim, J.H., Cho, H.I., Park, H.J. and Kim, D.S. (2017), “Evaluation of soil state variation using bender elements within centrifuge models”, *Geotech. Test. J.*, **40**(1), 150-159.
<https://doi.org/10.1520/GTJ20150139>.
- Kim, N.R. and Kim, D.S. (2010), “A shear wave velocity tomography system for geotechnical centrifuge testing”, *Geotech. Test. J.*, **33**(6), 434-444.
<https://doi.org/10.1520/GTJ102894>.
- Leonards, G.A. and Frost, J.D. (1988), “Settlement of shallow foundations on granular soils”, *J. Geotech. Eng.*, **114**(7), 791-809.
[https://doi.org/10.1061/\(ASCE\)0733-9410\(1988\)114:7\(791\)](https://doi.org/10.1061/(ASCE)0733-9410(1988)114:7(791)).
- Lo Presti, D.C.F. (1989), “Proprietà dinamiche dei terreni [Dynamic properties of soils]”, *Proceedings of the 14th Conference on Geotechnics Torino*, Department of Structural Engineering, Politecnico di Torino, Turin, Italy (in Italian).
- Martin, C.L., Bouvard, D. and Shima, S. (2003), “Study of particle rearrangement during powder compaction by the discrete element method”, *J. Mech. Phys. Solids*, **51**(4), 667-693.
[https://doi.org/10.1016/S0022-5096\(02\)00101-1](https://doi.org/10.1016/S0022-5096(02)00101-1).
- Mayne, P.W. and Kulhawy, F.H. (1982), “ K_o -OCR relationships in soil”, *J. Soil Mech. Found. Div.*, **108**(6), 851-872.
- Mayne, P.W. and Poulos, H.G. (1999), “Approximate displacement influence factors for elastic shallow foundations”, *J. Geotech. Geoenviron. Eng.*, **125**(6), 453-460.
[https://doi.org/10.1061/\(ASCE\)1090-0241\(1999\)125:6\(453\)](https://doi.org/10.1061/(ASCE)1090-0241(1999)125:6(453)).
- Mesri, G. and Vardhanabhuti, B. (2009), “Compression of granular materials”, *Can. Geotech. J.*, **46**, 369-392.
<https://doi.org/10.1139/T08-123>.
- Mir, M., Bouafia, A., Rahmani, K. and Aouali, N. (2017), “Analysis of load-settlement behaviour of shallow foundations in saturated clays based on CPT and DPT tests”, *Geomech. Eng.*, **13**(1), 119-139.
<https://doi.org/10.12989/gae.2017.13.1.119>.
- Roesler, S.K. (1979), “Anisotropic shear modulus due to stress-anisotropy”, *J. Geotech. Eng. Div.*, **105**(GT7), 871-880.
- Schanz, T., Vermeer, P.A. and Bonnier, P.G. (1999), *The Hardening Soil Model: Formulation and Verification*, in *Beyond 2000 in Computational Geotechnics*, 281-296.
- Schmertmann, J.H. (1970), “Static cone to compute static settlement over sand”, *J. Soil Mech. Found. Div.*, **96**, 1011-1043.
- Schmertmann, J.H., Brown, P.R. and Hartman, J.P. (1978), “Improved strain influence factor diagrams”, *J. Geotech. Eng. Div.*, **104**, 1131-1135.
- Tasiopoulou, P., Taiebat, M., Tafazzoli, N. and Jeremic, B. (2015), “On validation of fully coupled behavior of porous media using centrifuge test results”, *Coupled Syst. Mech.*, **4**(1), 37-65.
<http://dx.doi.org/10.12989/csm.2015.4.1.037>.
- Umar, M. and Sadrekarimi, A. (2016), “Accuracy of determining pre-consolidation pressure from laboratory tests”, *Can. Geotech. J.*, **54**(3), 441-450. <https://doi.org/10.1139/cgj-2016-0203>.
- Yoon, H.K., Lee, C., Kim, H.K. and Lee, J.S. (2011), “Evaluation of preconsolidation stress by shear wave velocity”, *Smart Struct. Syst.*, **7**(4), 275-287.
<http://doi.org/10.12989/sss.2011.7.4.275>.
- Yu, P. and Richart, F. (1984), “Stress-ratio effects on shear modulus of dry sands”, *J. Geotech. Eng. Div.*, **110**(3), 331-345.
[https://doi.org/10.1061/\(ASCE\)0733-9410\(1984\)110:3\(331\)](https://doi.org/10.1061/(ASCE)0733-9410(1984)110:3(331)).

GC